iJRASET
International Journal For Research in Applied Science and Engineering Technology

INTERNATIONAL JOURNAL FOR RESEARCH

IN APPLIED SCIENCE & ENGINEERING TECHNOLOGY

Volume: 10 **Issue:** VI **Month of publication:** June 2022

DOI: https://doi.org/10.22214/ijraset.2022.44613

www.ijraset.com

Call: 08813907089 | E-mail ID: ijraset@gmail.com

International Journal for Research in Applied Science & Engineering Technology (IJRASET)
ISSN: 2321-9653; IC Value: 45.98; SJ Impact Factor: 7.538
Volume 10 Issue VI June 2022- Available at www.ijraset.com

A Segmentation Process to Isolate Various Cytological Components from Follicular Histology based on Texture Heterogeneity

Pranshu Saxena[1], Anjali Goyal [2]
[1]*IK Gujral Punjab Technical University, Kapurthala,India*
[2]*Guru Nanak Institute of Management and Technology, Ludhiana, India*

Abstract: ***This research looks at an H&E-stained Follicular Lymphoma tissue sample in order to isolate different cytological components based on textural heterogeneity. The goal of this study is to determine the morphological behavior of various cytological components such as nuclei, cytoplasm, extracellular material, and red blood cells so that oncologists can make better decisions and provide appropriate treatment during the prognosis of histopathological images that are sometimes incorrectly concluded. To isolate these cytological components, a convolution process is applied to follicular histology and 8 different oriented masks produced from the gabor filter, yielding 8 separate representations for each of the 8 various orientation masks of H&E-stained FL histology. The information included in the 8 representations resulting from the application of the gaussian filter is summarized in twelve images that correspond to each of the filter's orientations. Second, the operation of concatenation is carried out over these 8 separate representations into a single 3-dimensional covariance image. The projected approach outperforms grey level-based texture analysis in FL histology, according to the results.***
Keywords: Computer-aided diagnosis, follicular lymphoma, gabor mask, gaussian wavelet, image classification, texture analysis.

I. INTRODUCTION

Follicular lymphoma (FL) is a type of non-Hodgkin B-cell lymphoma that has a variety of clinical outcomes. Patients with Aggressive FL have a short survival time if they are not treated early and efficiently, thus they should begin therapy as soon as possible to improve their chances of remission and lengthen their lives. These crucial clinical decisions are now guided by the cancer's histology grading. The number of large malignant cells, known as Centroblasts (CB), per standard 40 magnifications high power microscopic field (HPF) of 0.159 mm^2 is used by the World Health Organization (WHO) for histological grading of FL [1] [21]. Centroblasts are manually counted and the CB/HPF [7] average is calculated in this approach. According to the WHO, the average CB count per HPF of hematoxilin and eosin (H&E) stained tissue sections (under microscope) is used to categories the biopsy into one of three histopathological grades. Grades I and II (0–5 CB/HPF) are low-risk categories, whereas Grade III (>15 CB/HPF) is a high-risk category. The clinical use of the grading system is still being contested; Grades I, II, and III/A are considered indolent and incurable, but Grade III/B is the most aggressive yet treatable [16]. Grades I and II in the aforementioned classification are quantitative issues (count the number of CB/HPF), however Grade III in its respective subgroups is a qualitative issue (CB/HPF stay the same (>15 in both Grade III A and B). The only subjective difference between Grade IIIA and B is that in IIIA, centrocytes are still present, but in IIIB, the follicles are nearly totally made up of Centroblast [16], [21]. Although patients with indolent FL (Grade I, II, and III) might survive for decades with little or no therapy, patients with aggressive FL have a shorter life expectancy if not treated properly at an early stage. In the current scenario, pathologists often count CBs that may be probable repercussions of over or under grading of FL, such as improper timing and kind of medication, which can have major clinical implications for patients. Furthermore, the precision of the categorization is critical in order to avoid under or overtreatment. Unfortunately, when oncologists prognosticate these highly microscopic (e.g. 40x) biopsy by only selecting a small representative section (e.g. 2x or 4x) and concluding for a whole slide (40x) tissue sample, this classification becomes more vulnerable, and sometimes subjectivity issues arise among different readers. The subjectivity and inconsistency of manual grading has an impact on diagnostic accuracy and treatment success. Therefore, this paper is focusing on to provide distinguished representation for each element (nuclei, cytoplasm, extracellular material and red blood cell) from H&E-stained input image so that subjectivity between oncologists can be reduces. Proposed algorithm is able to represent each Centroblastic elements of FL image with different color. Because of the differences in colour representation, a new quality measure called texture analysis is created, which refers to the categorization of regions in an image based on their texture content.

Texture analysis aims to quantify perceptual features such as rough, smooth, silky, or bumpy as a result of spatial variation in pixel intensities, as well as to determine boundaries between major texture regions. Statistical approaches (grey level co-occurrence matrix, grey level difference vector), filtering techniques (energy filters), wavelet decomposition-based methods, and so on are all utilised to extract features.

This work focusing on assessing some of the gabor function application strategies for the characterization of textures that generate many different kinds of environments for histopathological image, by observing each component of image with all conceivable angles and plotting a 3-D image. This method differs significantly from the scheme proposed by S. Kothari et al. 2013 [20], which used a shaped-based feature to classify lymphomas into grades. The rest of the paper is organized as follows: Section II describes proposed methodology; Section III describes about automated texture analysis methodology. In Section IV, experimental results followed by discussion with three experienced pathologists is presented, and finally, in the Section V, conclusion and future scope is discussed followed by future aspect of research work.

II. PROPOSED METHODOLOGY

The tests were performed using two images FL and the samples are collected from the various pathology in India First, Medicare Pathology Laboratory, Pune, Second, Dr. Girishs Trividi cancer Centre, kharghar (Navi Mumbai) and Finally Dr. Rubi pathology & Medical Centre, Jhansi. We asked three experienced pathologists to extract five regions of interests from each whole-slide sample that are equivalent to one microscopic HPF, resulting in a data set of 170 images. Texture features are extracted from the image using MATLAB, on Windows 10, Intel Processor.

Actually, texture is the intuitive property of surface, no strict definition about image texture, it only perceives by humans and is believe to be rich source of visualization. Rosenfeld et al. [9] defines texture in terms of image property like brightness, color, contrast, entropy, mean, size, slope, and complex visual patterns composed by image elements (sub patterns). Consider an image $I : \Omega \rightarrow R$, Ω is the image domain and the segmentation of the image into its subsequent region R is depends on the local sub patterns visual property like lightness, uniformity, density, roughness, regularity, smoothness, randomness, frequency, phase, granularity etc. as a whole Levine et al. [10] introduced that by localizing the image criteria.

Most common multi-scale feature technique that has been widely uses are texture discrimination and texture classification. Based on these classifications a lot of texture segmentation methods has been introduced by distinguished researchers, are as follows;

L. Cohen el.al [12] suggested a method rely on frequency that has been used for calculating these multi scale features. The most frequently used features are Wigner distribution, Gaussian Wavelet transformation, and Gabor application; however, Wigner distribution are found to hold interference terms between different components of a signal, means little but significant variation does not affect the final outcome, resultant wrong interpretation of specified object (signal). Gabor filter are criticized for their non-orthogonally i.e. convolution between image and the filter bank are not correlated, this results information contained in Gabor image representation redundant and also affect the size of representation channels Teuner et al. concluded that [11].

Gabor filters are still employed for texture segmentation [11], [12], [13], [14], [15], [17], and [19] discuss the challenges of constructing gabor filters for texture segmentation. The wavelet transformation, on the other hand, is a linear operation that does not create interference terms, unlike the wigner distribution. It has the capacity to spatially localize signal (energy propagating via image) spectral features.

As a result, there has lately been a lot interest in wavelet transform applications in texture analysis. In a subsequent discussion, we provide a wonderful multi-resolution strategy (based on the aforesaid parameters) for segmentation the texture from colour medical image using the gabor application.

III. AUTOMATED TEXTURE ANALYSIS

Because it imitates the characteristics of the human visual system, which decomposes the image on the retina into several filtered images, each of which has variation in intensity with in a limited range of orientations and frequency [13], the multi-oriented filter is an effective method in the field of texture analysis. Furthermore, in most research, the relationship to the local spectrum is created by (intermediate) features acquired by filtering the input image with a series of 2-D gabor filter, such as linear and local filters. A gaussian and a cosine function are combined to form the convolution kernel.

In this paper a multi-oriented Gaussian filter banks (eq. 1) is implemented, which comprises of 8 different filters having different angles ranging from (450-3600). The particular characteristic of passing input H&E-stained image from every filter bank, resulting 8 different convolved images corresponding to each angle, each of the image represent its own site of view (figure.1). Later on, merging of all 8 convolved images into a single covariance image Time-varying 2-D histopathological images can be converted to

3-D space-time functions in this way, and time-varying images can be represented in vision areas by a 3-D Gabor-wavelet transform, which generates a time-varying five-dimensional field (representing two spatial dimensions, spatial frequency, spatial orientation, and temporal frequency) (MacLennan 1997, p. 64). The texture's orientation is a trait whose examination is often of importance for visualizing different intensities and using image classification.

As a consequence, the classification results generated by summing the output images from filtering with the eight filters according t o a defined orientation were put to the test.

$$G(\text{mask}) = G45° + G90° + G135° + \cdots\ldots + G360° \quad \ldots\ldots(1)$$

This above formula illustrates compete filter bank comprises of 8 mask having different angles. Implementation of mask, which depends on orientation, is explained below. A gabor filter is a complicated Gaussian exponential function modulated by a sinusoidal curve in the spatial domain.

$$G(x,y) = \frac{1}{2\pi\sigma^2}\exp\left[-\frac{x^2+y^2}{2\sigma^2}\right]\exp\{J(2\pi F(x\cos\theta + y\sin\theta))\} \quad \ldots\ldots(2)$$

In the spatial domain, represents a spatial extension of the mentioned filter. eq. 2 is divided into their respective real and imagery part. Oscar & Rafael suggested that only real part is necessary to represent and reconstruct the image [10] and that can be achieved by making theoretically DC (zero frequency) response of the real part of our 2D-gabor filter is closed but not exactly zero. Thus imposing zero frequency on them.

$$Re(x,y) = \frac{1}{2\pi\sigma^2}.\exp\left[-\frac{x^2+y^2}{2\sigma^2}\right].\cos((2\pi(a_0x + b_0y)) \quad \ldots\ldots(3)$$

$$Img(x,y) = \frac{1}{2\pi\sigma^2}.\exp\left[-\frac{x^2+y^2}{2\sigma^2}\right].\sin((2\pi(a_0x + b_0y)) \quad \ldots\ldots(4)$$

Here, a_0, b_0 define the spatial frequencies

$$\text{Magitude } F_0 = \sqrt{a_0{}^2 + b_0{}^2} \quad \ldots\ldots(5)$$

$$\text{Direction } \theta = \tan^{-1}\left(\frac{b_0}{a_0}\right) \quad \ldots\ldots(6)$$

Now, consider the eq.3 which consists of an exponential function along with three variables σ (spatial extension), and a_0 & b_0 these spatial frequencies can be represented in the terms of orientation θ & F0 easily ($a_0 = F_0\text{Cos}\theta$, $b_0 = F_0\sin\theta$).

As a consequence, the final result included eight orientations (45°,90°,135°,180°,225,270°,315°,360°) and one radial frequency value: F0= (0.3536). Now a total of eight filters that span the whole frequency range. Different standard deviation values of the Gaussian curve were evaluated (Chan, et al. 1999) [18], with g = (1.91, 3.82, and 7.63) and g = (1.91, 3.82, and 7.63) being the two sets of three values employed in the study (2.86, 5.73 and 11.44). These values aid in the creation of the Gabor mask.

The Gabor mask is built using eq. 3 of the real component of a complex exponential function, with each mask consisting of real Eigen values. Following the creation of the mask, the methodological technique for extracting texture variables and later image classification was as follows (fig. 1), which briefly describes the development of the textured image.

The Gabor Filter provides information on the orientation and frequency of the features. Frequency is fixed and predetermined but different orientations of an image's texture is calculated because an image is filtered with a set of Gabor filters of different preferred orientations and spatial frequencies that cover appropriately the spatial frequency domain, and the features obtained from a feature vector field that is further used for analysis, classification, or segmentation.

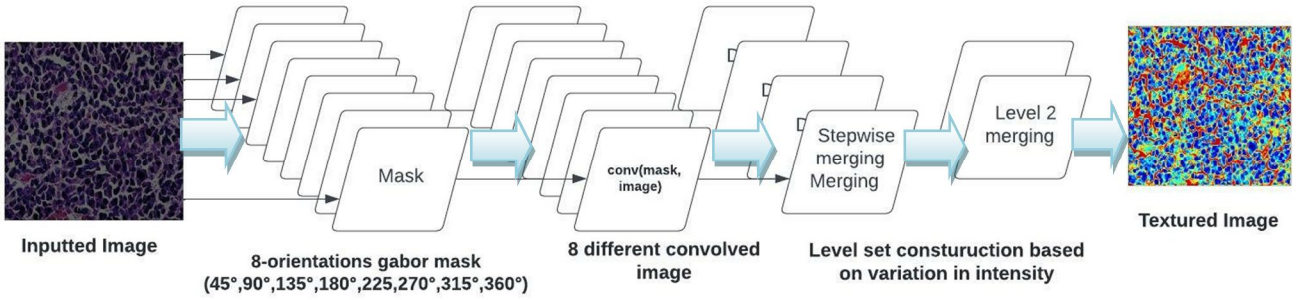

Fig. 1. Process flow for getting output textured Image

We are these following ways to achieve our final textured image;
Input Image
Let Ω be the colour medical image and $I : \Omega \rightarrow R$ be the image domain. By charting each cytoplasmic element with a distinct hue, picture I may be segmented. The image $I(x,y)$ is a spatial representation of the picture, where (x,y) is the set of all points in the domain; we must load the H&E-stained image and do the necessary conversions.

A. Gaussian Filters
We construct 8 different masks (having $45°$ with respect to each other) with the help of Gabor application;

$$\mathcal{G}_{(\theta,\sigma,F_0)} = \frac{1}{2\pi\sigma^2}\exp\left[-\frac{x'^2 + y'^2}{2\sigma^2}\right].\cos\left((2\pi(a_0x' + b_0y')\right) \quad \ldots\ldots(7)$$

In this formulation

$$x' = (x-\xi)\cos\theta - (y-\eta)\sin\theta \quad \ldots\ldots(8)$$

$$y' = (x-\xi)\sin\theta + (y-\eta)\cos\theta \quad \ldots\ldots(9)$$

Where, x and y belongs to the coordinate position of a point in spatial domain and ξ, η, θ, σ, F_0 are the parameters whose modification changes the Gabor mask formulation. The centre of an interested field is specified by parameter (ξ & η), which has the same domain Ω as a pair of (x, y), parameter accounts for the size of the interested field, and the angle parameter θ $\left(\theta \in [0,2\pi)\right)$ determines the orientation of the normal to the parallel excitatory and inhibitory strips zone.
This formula generates eight separate Gabor masks; these masks are then applied to the input image, and the magnitude of the filtered images is calculated. Finally, we convolve our input image with each of the eight masks to get eight different view angle images.

B. Convolution Procedure
With the help of Gabor application, we created 8 different 2-D Gabor masks $\mathcal{G}(x,y), (x,y) \in \Omega$, we convolved our input image $I(x,y)$, to get a gabor featured image $r(x,y)$ as follows;

$$r(x,y) = \iint_{\Omega} I(\xi,\eta) * g(x-\xi, y-\eta) \quad \ldots.(10)$$

This formulation gives us 8 different representations of inputted image, corresponding to each angle discuss in eq. 2 and each of the element (cytoplasmic) which image consists of, have all possible view angle representation ($45°$ to $360°$). This way we are able to plot every cytoplasmic element in 3-D representation. The magnitude image was then passed through a Gaussian low-pass filter to reduce its variance and, as a result, the classification error.

C. Combining all Convolved Images

The outputs of convolving procedure in each image point can be combined in a single quantity (textured image) that is called Gabor energy. That energy simply formulated by finding out final covariance matrix from all convolved images. This feature is related to the model of a specific type of orientation selective neuron in the primary visual cortex and is defined in the following way;

$$\mathcal{G}_{\text{energy}(L_{1i})} = \sum_{i=2p+1}^{8} C_i(j) * C_{i+1}(k+1-j) \quad \ldots\ldots(11)$$

This formulation accounts for all the covariance matrix which we for convolved in level 1 step 4 (figure 1) eq. 12 returns 6 covariance matrix form 12 convolved images. In the level 2 step 5 (figure 1) we repeat this process until we get final covariance image. Where, $p = 0,1,2, \ldots ,5$ i.e. i will keep track all convoluted images $(1 \text{ to } 8)$. Let m is the length of C_i and n is the length of C_{i+1}, then the length of $\mathcal{G}_{\text{energy}}$ $m+n-1$ whose Kth element is displayed in eq. 12 and the sum is over all the values of j which lead to legal subscripts for $C_i(j)$ and $C_{i+1}(k+1-j) : \min(k,m)$. When $m = n$.Next two steps can be formulated as follows;

$$\mathcal{G}_{\text{energy}(L_{2i})} = \sum_{i=2p+1}^{6} L_{1i}(j) * L_{1(i+1)}(k+1-j) \quad \ldots\ldots(12)$$

Where, $p = 0,1,2$ i.e. i will track all convoluted image$(1 \text{ to } 6)$

$$\mathcal{G}_{\text{energy}(L_{3i})} = \sum_{i=2p+1}^{3} L_{2i}(j) * L_{2(i+1)}(k+1-j) \quad \ldots\ldots(13)$$

Where, $p = 0,1$ i.e. i will track all the convoluted images $(1 \text{ to } 6)$ and finally, we Conquer all these convoluted images (from convolution process) in the one covariance matrix (classification) this entire process gives us final segmented image. The filtered images were used as variables or texture bands in a supervised classification procedure using the maximum likelihood approach.
So the figure 2 shows the abstract view of all the process which leads us to concluded texture image.

This all process can we judge by this mathematics;

$$\text{Final Textured Image} = \text{covn}^1[\sum_{i=1}^{8} IM * GM_i] \quad \ldots\ldots(14)$$

Where IM = input image that would remain constant until the final corresponding (Texture) image, (*) convolution operator, GM = Gabor mask (eq. 1), covn defines that final outcome contains final covariance matrix. Later part shows the discussion with doctors (only subjectivity). In the next paper we try to proof grading analysis (I, II, III), means in which grade our input image lies and compare it by doctor's prognosis regarding grading.
Later this textured image has been passed from level set formulation phase where these differences among intensities are plotted with different color in the purpose of segmenting each cytoplasmic element distinctly. This level set formulation deforms iteratively to partition the image into region. Main idea behind this approach is that to distinguish background and fore ground (biased region and cytoplasmic part). In this level set frame work, contour C is in 2-Dimensional plane (coming from Gabor application) simple embedded in a 3-Dimensional surface ϕ, this ϕ will track inside $(\phi < 0)$ and outside $(\phi > 0)$ when ϕ crosses a plane at the 0 level. This ϕ is chosen to be the signed distance function such that; the $|\phi|$ is equal to the distance from x to the closest point on contour C and interior points have a negative sign. This choice is made so that we can cluster homogeneous intensities and distinguished on account of color, where intensity varies drastically.

IV. EXPERIMENTAL RESULT'S AND DISCUSSION

Using unsupervised segmentation, we partitioned the images into various cytological components to get the desired outcome. Nuclei, cytoplasm, background, red blood cells (RBCs), and extracellular material are the five key components of H&E-stained FL & NB pictures, and each of them is expressed in a different colour hue. We utilised the L*a*b* colour space for segmentation because the difference between two hues is perceptually consistent; hence, the Euclidean distance may be employed as a metric [6]. In figure 2 image (c) & (f) explains the amount of area coverage by each cytoplasmic component because this classification is needed at a time of prognosis of tissue sample.

Discussion with doctors leads us to know about the relevance of these cytoplasmic components in the occurrence of diseased grading. They suggested us any single tissue made up nuclei surrounded by cytoplasm, and usually nuclei is round in shape, but when the patients suffer from lymphomas, nuclei shape deteriorate (either reduce in size or become larger from actual), result more and less cytoplasm and nuclei occurrence in textured image. We have taken two images (figure 2 (a) & (d)) of follicular lymphoma grade II and III, respectively and in ours 170 images of database. Discussion with doctors helps us to understand each cytological component and plot each of them distinctly with different color.

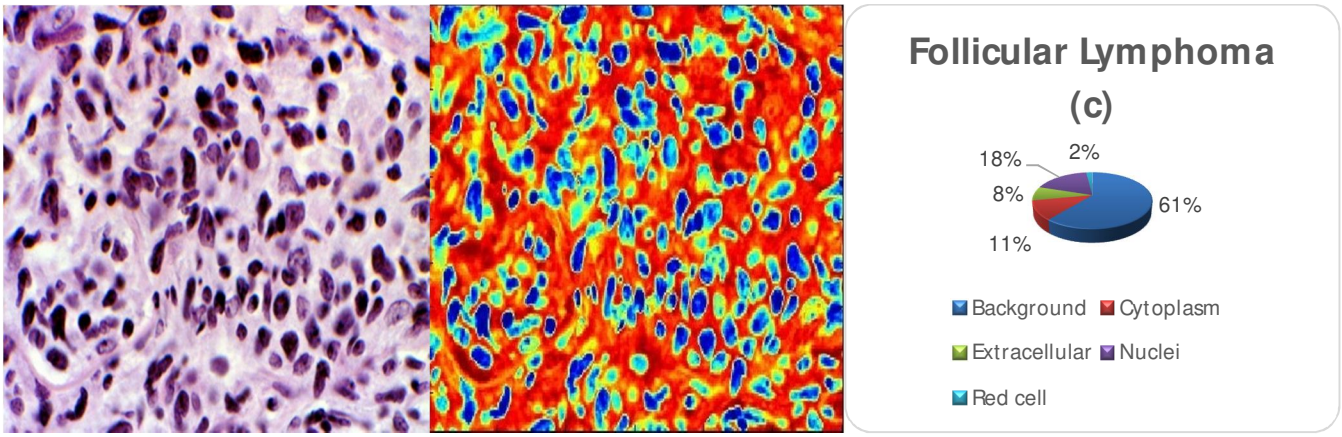

(a) (b) (c)

b)

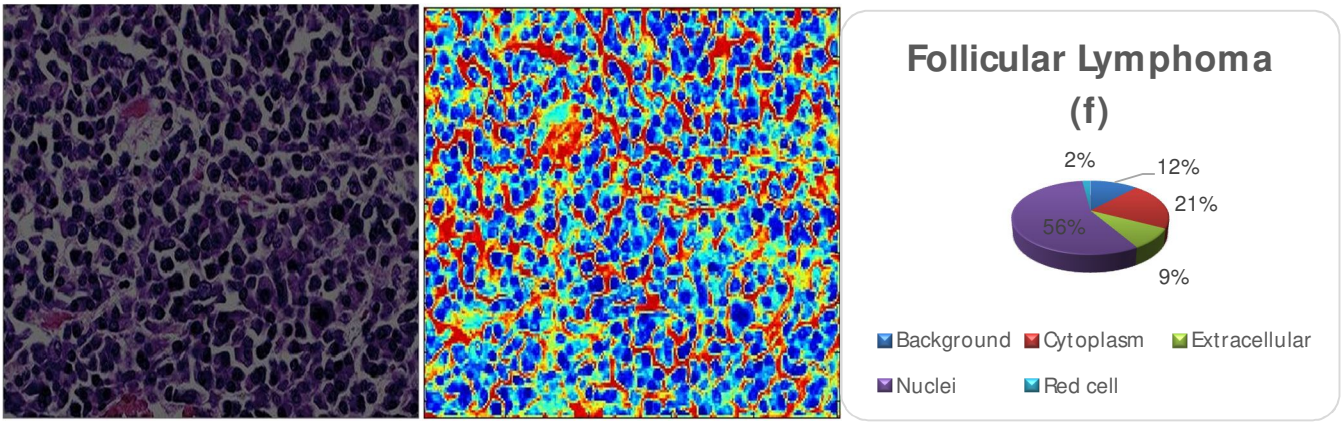

(d) (e) (f)

Fig. 2. (a) & (d) are the input images of Follicular Lymphoma Grade II & III respectively, (b) & (e) are the Textured image, (c) & (f) image shows amount of cytoplasmic component present in the final output image.

Though this discussion is confined to qualitative criterion of grading of Lymphomas, still this study can provide a healthy discussion regarding grading of lymphomas because in figure 2 (images (b) & (e)) quantized each cytoplasmic component, level set formulation maintain a lists for accounting each cytoplasmic element separately. This quantization provides doctors additional input with minimal cost help to make efficient decision timely and also helps in the categorization into respective grades as CB/HPF ratio can we visualized.

Sample H&E-stained images (shown in figure 2 (a) & (d)) and their segmentation (Textured) results (shown in figure 2 (b) & (e)) of Follicular Lymphoma, each color represent its own identity blue corresponds to nuclei, cyan to cytoplasm yellow to extracellular and red and gray to background and red cells, respectively. We could also able to differentiate the low intermediate and high grades (CB/HPF) with reasonable accuracies.

In previous researches segmentation based on color [8] are not much more effective for the image having high CB/HPF ratio the displayed it outcomes in gray scale (black & white). Those out comes hardly justify our grading scheme of H&E-stained histopathological image.

V. CONCLUSION

We developed a unique colour texture analysis method and used it to help in the diagnosis of follicular lymphoma images. Prior to Co-occurrence computation for H&E-Stained histopathology image, Gaussian wavelet orientation modification of colour images significantly enhanced classification performance, with 97% in sensitivity in diagnosing follicular lymphoma according to pathologist. In histopathology images of FL, our suggested technique shows tremendous potential in establishing structure, color-textural, and structural information. Furthermore, our categorization technique provides extra information to pathologists, allowing patients to receive proper treatment as soon as feasible, increasing their chances of remission and living longer.

It is important to highlight that an automated computer assisted grading system should never be used in place of a pathologist. Instead, it should only be utilized to aid the decision-making process. We shall witness following scenarios in the future. The suggested color texture analysis technique will be tested to see whether it can be used to analysis other types of images with a limited colour range. To count the number of nuclei and other centroblast element present in any image, as well as to designate them appropriately fro visualization.

REFERENCES

[1] Jaffe, E.S., Harris, N.L., Stein, H., and Vardiman, J.W., "Tumors of Hematopoietic and Lymphoid Tissues", IRAC Press, Lyon, 2001.
[2] Clausi, D.A & M.E. Jernigan, "Designing Gabor filters for optimal texture separability". Pattern Recognition. Vol. 33, pp. 1835-1849, 2000.
[3] Bovic, A.C., 1991. "Analysis of multichannel narrowband filters for image texture segmentation". IEEE Transactions on signal processing. Vol. 39 no. 9, pp. 2025-2043, 1991.
[4] G. Paschos, "Perceptually Uniform Color Spaces for Color Texture Analysis: An Empirical Evaluation," IEEE Trans. On Image Processing, pp. 932-937, 2001.
[5] Jorge A. Recio, Luis A. Ruiz Fernan, "Use of Gabor filters for texture Classification of digital images" ISSN: 0214-4557.Física de la Tierra, vol. 17, pp. 47-59, 2005.
[6] Oscar Nestares, Rafael Navarro, Javier Portilla and Antonio Tabernero , "Efficient Spatial-Domain Implementation Of A Multiscale Image Representation Based On Gabor Functions," J electronic imagining vol. 7, pp. 166-173, 1998.
[7] Swerdlow, S., Campo, E., Harris, N., Jaffe, E., Pileri, S., Stein, H., Thiele, J., and Vardiman, J., eds., "WHO classification of tumours of haematopoietic and lymphoid tissues", vol. 2, World Health Organization, Lyon, France, fourth ed. (2008).
[8] Amanpreet Kaur Bhogal, Neeru Singla, Maninder Kaur, "Color Image Segmentation Based On Color And Texture properties", international journal of advanced engineering sciences & technologies vol no.8,issue no.2,152-156.
[9] A. Rosenfeld and A. Kak, "Digital picture Processing," vol. 1, Academic Press, 1982.
[10] M. Levine, "Vision in Man and Machine," McGraw-Hill 1985.
[11] A. Teuner, O. Pichler and B. Hosticks, "Unsupervised Texture Segmentation of Images Using Tuned Matched Gabor Filter," IEEE Transaction Image Processing vol. 4 no. 6, pp. 863-870, 1995.
[12] P. Cohen, C. Ledinh and V. Lacasse, "Classification of Natural Texture by Means of Two-Dimensional Orthogonal Masks," IEEE transaction Acoustic, Speech and Signal Processing, vol. 37 no. 1, pp. 125-128, 1989.
[13] A. Jain and F. Farrokhnia, "Unsupervised Texture Segmentation Using Gabor Filters," Patterns Recognition, vol. 24 no. 12, pp. 1167-1186, 1991.
[14] D. Dunn, W. Higgins and J. Wakeley, "Texture Segmentation Using 2-D Gabor Elementary Function," IEEE transaction Patterns Analysis and Machine Intelligence, vol. 17 no. 2 pp. 130-149, 1994.
[15] J. Bigun and J. du Buf, "N-folded Symmetries by Complex Moments in Gabor Space and Their Application to Unsupervised Texture Segmentation," IEEE Transaction Patterns Analysis and machine Intelligence, vol. 16 no. 1 pp. 80-87, 1994.
[16] G. Anneke, B. Bouwer, G. W. Imhoff, R. Boonstra, E. Haralambieva, A. Berg, B. jong, " Follicular Lymphoma grade 3B includes 3 cytogenetically defined subgroups with primary t(14;18), 3q27, or other translations: t(14;18) and 3q27 are mutually exclusive" blood journal hematology library, Feb. 2013.
[17] D. Dunn and W. Higgins, "Optimal Gabor Filters for Texture Segmentation," IEEE transaction on Image processing vol. 4 no. 7, pp. 947-964, 1995.
[18] T. Chan and L. Vese, "Active contours model without edges," IEEE transaction Image Processing, Vol. 10, no. 2, pp. 266-277, Feb. 2001.
[19] Pranshu Saxena and Sanjay K. Singh, "Noble Approach for Texture Classification of H&E-Stained Histopathological Image by Gaussian Wavelet," IEEE symposium intelligent system designs (ISDA) pp. 323-327 Nov 2012.
[20] Sonal Kothari, John H Phan, Andrew N Young and May D Wang, "Histological image classification using biologically Interpretable shape-based features," Kothariet al. BMC Medical Imaging, 2013.
[21] Saxena, P., & Goyal, A.. Study of Computerized Segmentation & Classification Techniques: An Application to Histopathological Imagery. Journal of Computing and Informatics, 43(4), 561-572. https://doi.org/10.31449/inf.v43i4.2142 2019.

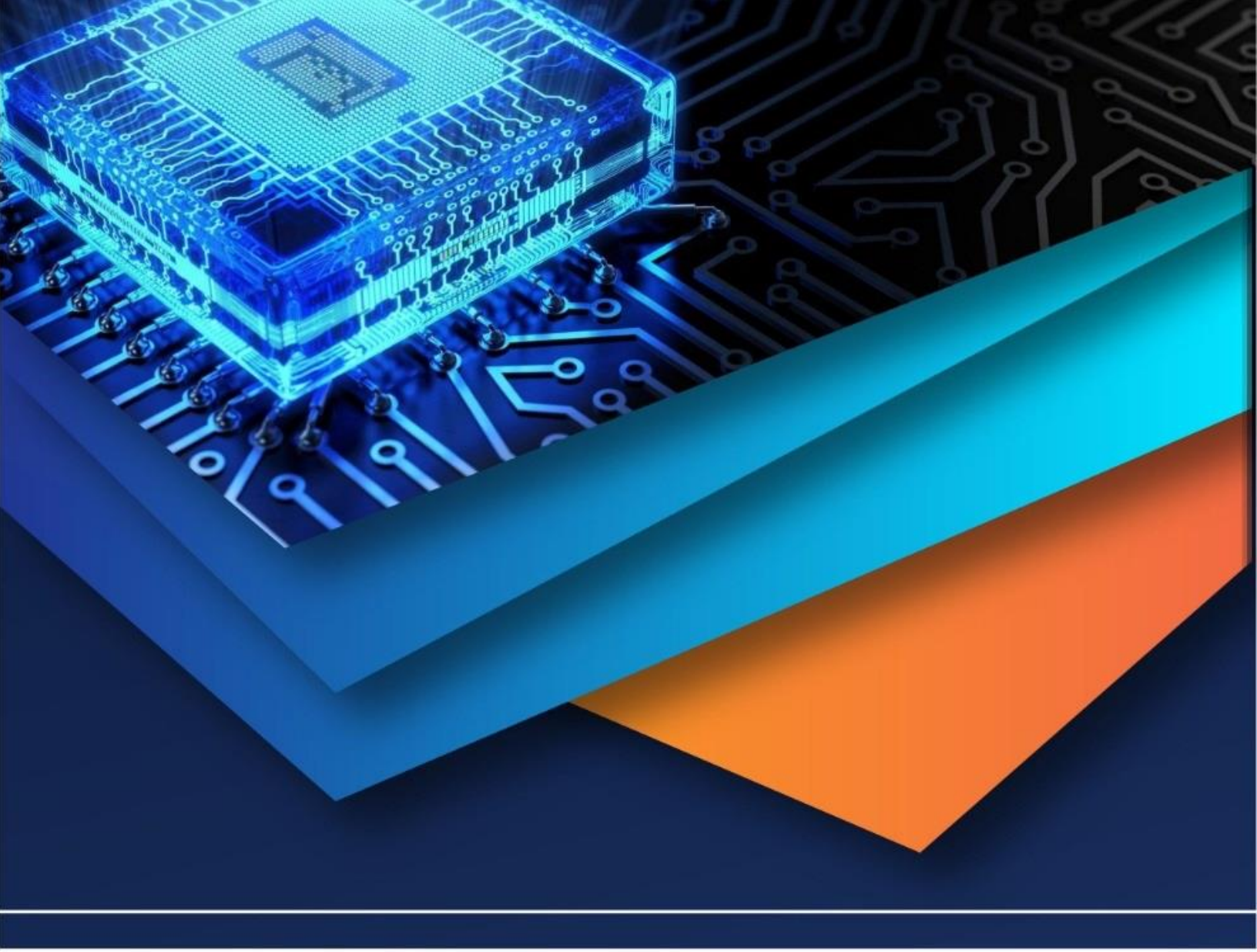

10.22214/IJRASET

45.98

IMPACT FACTOR: 7.129

IMPACT FACTOR: 7.429

INTERNATIONAL JOURNAL FOR RESEARCH

IN APPLIED SCIENCE & ENGINEERING TECHNOLOGY